Proceedings of the 17th World Congress
The International Federation of Automatic Control
Seoul, Korea, July 6-11, 2008

Model-based Predictive Control for the Exhaust Gas Cycle of an Oxyfuel-Process

Th. Nötges, S. Hölemann, D. Abel

Institute of Automatic Control, RWTH Aachen University, Aachen, Germany (e-mail: Th.Noetges@irt.rwth-aachen.de, S.Hoelemann@irt.rwth-aachen.de, D.Abel@irt.rwth-aachen.de).

Abstract: The global environmental warming which is discussed these days is, at the opinion of many experts, amongst other things ascribed to human induced carbon dioxide emissions which intensify the greenhouse effect. To face and overcome the negative consequences like environmental disasters, the rising mean sea level and others, new power plant concepts are researched and developed. In this article a novel, zero emission, oxyfuel power plant concept is discussed. Due to the novelty of the process it is examined in calculations, simulations and laboratory tests by a research group at RWTH Aachen university and does not exist in reality by now. Besides a conventional water cycle, an exhaust gas cycle has a major function in the process. The operation of the exhaust gas cycle requires an automation concept. In this paper an object-oriented model is used as a basis for examining the process behaviour and developing a controller for the multivariable and strongly coupled system. For the sliced exhaust gas cycle a model-based predictive controller is introduced. A parameter study presents the impact of selected controller parameters.

Keywords: Model predictive and optimization-based control; Process modelling and identification; Modelling, operation and control of power systems; Control system design; Object oriented modelling;

1. INTRODUCTION

The currently observed global warming is inter alia implicated to human induced carbon dioxide emissions (see Houghton et al. (2001); BASC (2000)). The expected negativ impacts such as environmental disasters and the rising mean sea level yield amongst others to novel fossil power plants with carbon dioxide separation. One concept which is researched at RWTH Aachen university is based on the oxyfuel combustion methodology which uses pure oxygen or oxygenated exhaust gas for oxidizing the combustibles.

The combustion gas is gained via the exhaust gas cycle depicted in fig. 1. Parts of the exhaust gas from the combustion chamber are recirculated and oxygenated in the ceramic high temperature membrane. The exhaust gas blower conveys the combustion gas into the combustion chamber where it is used to burn the coal. Since the exhaust gas after the combustion chamber principally only consists of the species H_2O and CO_2 an economical carbon dioxide separation becomes possible.

For the oxygen extraction ambient air is compressed and preheated in the gas-gas heatexchanger. While passing the ceramic high temperature membrane oxygen diffuses from the air side to the exhaust gas side. The diffusion is driven by the membrane temperature and the oxygen partial pressure ratio between the air and the exhaust gas side (see also eq. 1). As it will be discussed in more detail in the next section, both variables are influenced by the angular velocities of the compressor and of the exhaust gas blower as well. The compressed and heated air is expanded in the turbine to partly regain the energy conducted for its compression.

Since the introduced process is part of a research project, it is yet not existing in reality. Several partners develop the fundamentals for building and operating the plant. This paper addresses the automation of the process, analyzing the relevant control aspects and implementing a first model-predictive control strategy. As a starting point a sliced exhaust gas cycle without recirculation is considered. Due to the lack of data a process model is examined.

2. PLANT MODEL AND SENSITIVITY MATRIX

The model of the sliced exhaust gas cycle (see fig. 1) was realized using the object-oriented modelling language MODELICA. The highly nonlinear overall model is based on the *ThermoPower* library (see Casella, Leva (2003)) which uses the standard MODELICA *Media* library (see Casella et. al. (2006)).

The *Media* library provides structures, functions and data to model mere and mixture fluids. By defining two independent states of a mere fluid, its state is fully defined. Possible state variables are temperature T, pressure p, specific enthalpy h, specific inner energy u, specific entropy s or density ρ. In the *Media* library intensive state variables are used. For fluid mixtures additionally the composition $\underline{\xi}$ must be given.

The *ThermoPower* library provides connectors (i. e. a fundamental class to uniformly connect components to

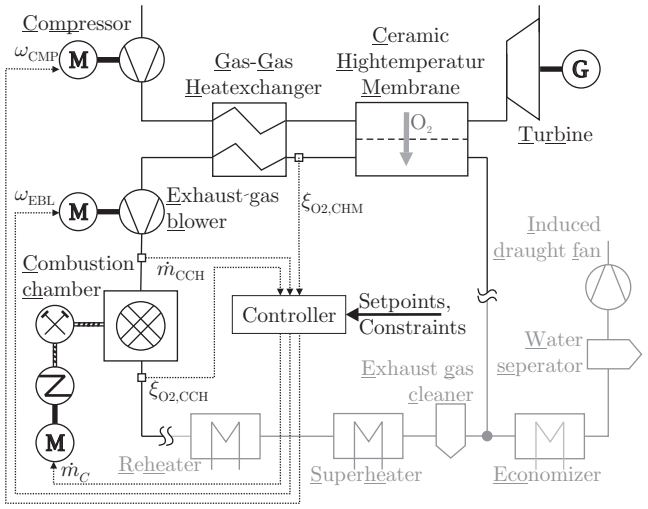

Fig. 1. Exhaust gas cycle of an Oxyfuel-Process with controller

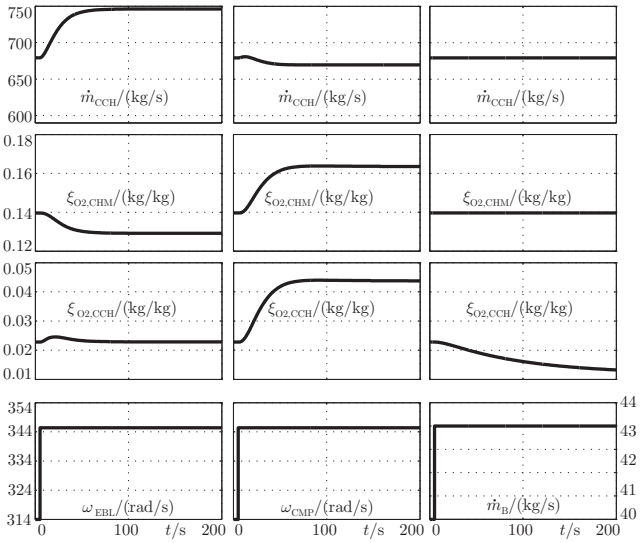

Fig. 2. Sensitivity study

each other) and basic models in the field of power plant modelling. Besides models for components on the water and (exhaust) gas side, thermal and electrical components are made available. An important basis of this library is the breakup between the conservation and state equations (see Casella, Leva (2003)). Thus, it is possible to formulate the components independently of the used fluid. Thereby, it is easy to exchange the fluid in an existing model.

For the turbo machines a characteristic number approach (see Gašparović (1973)) has been implemented and advanced [1] using the facilities of the modelling language. This approach is capable of estimating the static behaviour of axial turbo machines with only one set of equations using known or estimated design data. The dynamic behaviour is modelled using the principle of conservation of angular momentum.

For the ceramic membrane and the gas-gas heatexchanger a finite volume approach is used. The gas-gas heatexchanger is fully set up using the components of the *ThermoPower* library. Besides the heat conduction through the pipe walls, convection is considered as well as radiation. Simplified, the ceramic membrane can be illustrated as a heat exchanger augmented by the ability to transport oxygen. The basic equation for describing the diffusion

$$\dot{j}''_{O_2} = \frac{C_1}{d} T \exp\left(-\frac{C_2}{T}\right) \ln\left(\frac{p_{\mathrm{O_2,Air}}}{p_{\mathrm{O_2,Exhaust}}}\right) \qquad (1)$$

can be derived from an equation which was proposed by Wager (1975).

According to this the mass flow density $\dot{j}''_{O_2}$ (i. e. mass flow per area) depends on the two material constants C_1 and C_2, the layer thickness d the temperature T and the oxygen partial pressures $p_{\mathrm{O_2,Air/Exhaust}}$.

Special attention was drawn to the initialization of the process model. As the model consists of a complex set of nonlinear, differential algebraic equations (DAE), a consistent initialization is necessary (see Nötges et. al. (2007)). For this purpose adequate starting values have been assigned to the dynamic states as well as the iteration variables. Furthermore, the model was prepared to start in steady state.

The developed model is highly nonlinear and strongly coupled (see Nötges, Abel (2007)). Fig. 2 shows an excerpt of the accomplished sensitivity study clarifying the dynamics and the couplings between the in- and outputs. In the lowest row, the impressed inputs ω_{EBL} (angular velocity of the exhaust gas blower), ω_{CMP} (angular velocity of the compressor) and $\dot{m}_{\mathrm{C}}$ (coal mass flow into the combustion chamber) are given, the upper three rows show the corresponding system responses $\dot{m}_{\mathrm{CCH}}$ (exhaust gas mass flow into the combustion chamber), $\xi_{\mathrm{O_2,CHM}}$ (oxygen concentration behind the ceramic membrane) and $\xi_{\mathrm{O_2,CCH}}$ (oxygen concentration behind the combustion chamber).

When the angular velocity ω_{EBL} is raised the exhaust gas mass flow increases as expected. In consequence of the higher mass flow the oxygen concentration $\xi_{\mathrm{O_2,CHM}}$ decreases. However, the absolut oxygen mass flow ascends because of the lower ceramic membrane bulk oxygen partial pressure on the exhaust side which heightens the diffusion as a result of the higher driving partial pressure ratio (see eq. 1). This is why the oxygen concentration $\xi_{\mathrm{O_2,CCH}}$ rises.

The increase of ω_{CMP} leads to heightening both oxygen concentrations in consequence of the higher pressure, temperature and oxygen offer in the ceramic membrane and the higher oxygen diffusion. The exhaust mass flow first increases because of the higher diffusion. The higher temperature and intensified heat transfer on the air side cause a temperature rise on the exhaust side and hence a decrease in the density. At a constant rotational speed of the exhaust gas blower a smaller density - and hence a greater specific volume - causes the mass flow to decrease in the long term.

With a higher coal mass flow $\dot{m}_{\mathrm{C}}$ the oxygen concentration behind the combustion chamber decreases. In the sliced case introduced in this paper $\dot{m}_{\mathrm{CCH}}$ and $\xi_{\mathrm{O_2,CHM}}$ - in contrast to the closed exhaust gas cycle - are not effected.

[1] Simplifications of the original article as constant gas or geometric properties were overridden.

For a conventional PID-based automation, the discussed sensitivity matrix provides a reasonable basis to design a multivariable controller configuration. Furthermore, the matrix provides an informative basis to appreciate the behaviour of the model-based predictive controller. This is discussed in the next section.

3. SIMULATION ENVIRONMENT

The development of a model-based predictive controller (MPC) for the power plant and the simulations which produced the results of this article has been done with the tool MATLAB/SIMULINK®. Originally a coupling of the nonlinear MODELICA model with SIMULINK® was intended to verify the controller but failed so far due to technical problems. For primary analysis the nonlinear system formulated in MODELICA is therfore transformed to a linear system of order 63 using the linearization ability of DYMOLA. In the following, this linearized system description is used as the plant model in SIMULINK®. Further efforts will aim at controlling the nonlinear system.

In fig. 3 the structure of the developed SIMULINK® model is shown. The linear plant of order 63 is observed using a discrete Kálmán filter of order 12 (see also section 5). The conversion from continuous to discrete time domain is achieved with a sample and hold element. With the estimated state $\underline{\widetilde{x}}$ and the future setpoints $\underline{\widehat{w}}$ the MPC[2] calculates optimal values for the actuating variables $\Delta\underline{\widehat{u}}_k$ (see appendix A). In the next sections the controller requirements and the theoretical background are given.

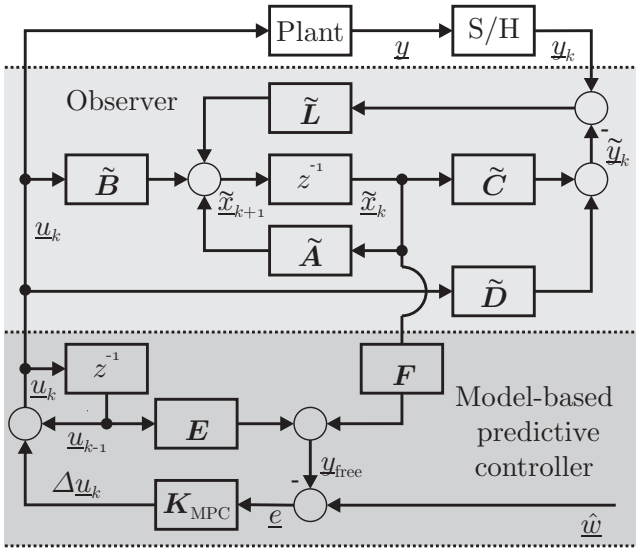

Fig. 3. Structure of the control circuit

4. CONTROLLER REQUIREMENTS

For the safe and efficient operating of the exhaust gas cycle it is necessary to control different variables. In this article three inputs and three outputs of the plant are considered (see fig. 1). As depicted in fig. 2 certain inputs are especially capable for controlling a certain output. In the following, the control variables are described and the preferred actuating variable is given.

First of all, the mass flow $\dot{m}_{\mathrm{CCH}}$ of the exhaust gas into the combustion chamber has to be controlled to handle power demands to the plant. A higher power demand generally requires more oxygen (contained in the exhaust gas) and coal carried into the combustion chamber. Currently, it is expected that the dynamic of the oxygen supply into the combustion chamber is slower than the dynamic of the coal supply. Hence, the setpoint for $\dot{m}_{\mathrm{CCH}}$ is raised to satisfy the power demand and $\dot{m}_{\mathrm{C}}$ is tracked to ensure the desired oxygen concentration after the combustion chamber. For regulating the mass flow ω_{EBL} is mainly used.

Second, the oxygen concentration $\xi_{\mathrm{O_2,CHM}}$ after the ceramic membrane has to be kept unchanged to assure constant and efficient combustion conditions even if other process parameters change. The burners, the combustion chamber and the steam generator will be optimized for the operating point and therefore depend on a constant $\xi_{\mathrm{O_2,CHM}}$. The regulation is mostly realized using ω_{CMP}.

Third, the oxygen concentration $\xi_{\mathrm{O_2,CCH}}$ has to be kept constant to assure complete combustion on the one hand and high efficiency on the other hand. The concentration behind the combustion chamber is a measure for the air/fuel ratio and therefore qualifies the combustion. $\xi_{\mathrm{O_2,CCH}}$ will be mainly regulated using $\dot{m}_{\mathrm{C}}$.

As mentioned earlier, the described system is a strongly coupled multivariable system. Furthermore, constraints exist for example for the rotational speed of the turbo components. To take the mentioned couplings and boundary conditions into account a model based predictive controller (MPC) will be applied. In this article a first concept is discussed based on a common discrete constrained linear MPC.

5. MODEL-BASED PREDICTIVE CONTROLLER

Below, a short summary on the predictive controller theory is given. A more detailed introduction can be found in Maciejowski (2002) or Rossiter (2003).

The functionality of the model-based predictive control concept is drafted in fig. 4.

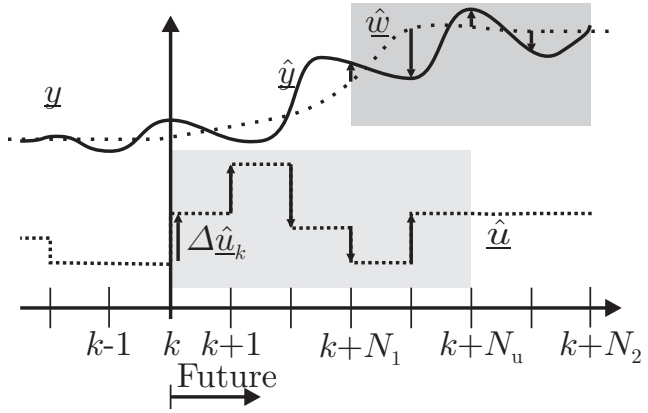

Fig. 4. Functionality of model-based predictive controllers

Model-based predictive controllers use an internal, in most cases simplified, dynamic model of the underlying control

[2] The same model of order 12 that is used for observation is used for the MPC, too.

process to estimate the prospective outputs $\widehat{\underline{y}}$ of the plant against values of the input signals $\widehat{\underline{u}}$ (see appendix A for the composition of the vectors). Applying process information in terms of a process model, MPCs are especially suitable for strongly coupled multivariable control systems like it is given with the exhaust gas cycle of the oxyfuel power plant. Furthermore an MPC provides the feasibility of feeding knowledge about future set points $\widehat{\underline{w}}$ (for example load requests) or disturbances to the controller. By minimizing the quadratic cost function

$$J = \left(\widehat{\underline{y}} - \widehat{\underline{w}}\right)^T \boldsymbol{\Gamma} \left(\widehat{\underline{y}} - \widehat{\underline{w}}\right) + \Delta\widehat{\underline{u}}^T \boldsymbol{\Lambda} \Delta\widehat{\underline{u}} \tag{2}$$

with

$$\widehat{\underline{y}} = \begin{pmatrix} \underline{y}_{k+N_1} \\ \vdots \\ \underline{y}_{k+N_2} \end{pmatrix}, \widehat{\underline{w}} = \begin{pmatrix} \underline{w}_{k+N_1} \\ \vdots \\ \underline{w}_{k+N_2} \end{pmatrix}, \Delta\widehat{\underline{u}} = \begin{pmatrix} \Delta\underline{u}_k \\ \vdots \\ \Delta\underline{u}_{k+N_u-1} \end{pmatrix} \tag{3}$$

an optimal trajectory of the actuating variables $\widehat{\underline{u}}$ is determined:

The cost function penalizes the squared sum of the deviations between the estimated future plant outputs $\widehat{\underline{y}}$ and the estimated future set points $\widehat{\underline{w}}$ and additionally the squared sum of the future control moves $\Delta\widehat{\underline{u}}$. $\boldsymbol{\Lambda}$ and $\boldsymbol{\Gamma}$ are weighting matrices (see eq. 4 to eq. 6). Thus, the operational behaviour is optimized under the expected future conditions. Moreover, MPCs are capable to handle constraints, for example given by limits of the controlled and actuating variables, by integrating them into the optimization problem. The optimization results in a trajectory of the actuating variables over the next N_u time steps. The inputs are assumed to remain constant for $k > N_u$. The optimization is repeated at every time step (receding horizon principle) and only $\widehat{\underline{u}}_k$ is applied to the plant.

The weighting matrix $\boldsymbol{\Gamma}$ which penalizes the deviation of each controlled variable for every time step in the predicted time period is composed by

$$\boldsymbol{\Gamma} = \begin{pmatrix} \boldsymbol{\gamma}_1 & 0 & \dots & 0 \\ 0 & \ddots & \ddots & \vdots \\ \vdots & \ddots & \ddots & 0 \\ 0 & \dots & 0 & \boldsymbol{\gamma}_{N_2-N_1+1} \end{pmatrix} \tag{4}$$

using the sub matrices $\boldsymbol{\gamma}_i$. The weighting matrix $\boldsymbol{\Lambda}^*$ for penalizing the use of the actuated variables is set up analogical using $\boldsymbol{\lambda}_i$. The matrices $\boldsymbol{\Gamma}$ and $\boldsymbol{\Lambda}^*$ are normalized such that

$$\sum_{i=1}^{N_2-N_1+1} \gamma_{i,i} = 100\,\% \text{ and } \sum_{i=1}^{N_u} \Lambda^*_{i,i} = 100\,\%. \tag{5}$$

The factor $S_{\frac{\boldsymbol{\Lambda}}{\boldsymbol{\Gamma}}}$ weights the penalization between control deviation and use of the actuated variables:

$$\boldsymbol{\Lambda} = S_{\frac{\boldsymbol{\Lambda}}{\boldsymbol{\Gamma}}} \boldsymbol{\Lambda}^*. \tag{6}$$

In the context of this article the process is abstracted to a linear system with three inputs $\underline{u}_k$ and three outputs $\underline{y}_k$. Using a discrete linear state-space description of the plant, the future outputs $\widehat{\underline{y}}$ can be computed within the lower $k = N_1$ and upper prediction horizon N_2 by eq. 7 [3].

$$\widehat{\underline{y}} = \boldsymbol{F}\underline{x}_k + \boldsymbol{E}\underline{u}_{k-1} + \boldsymbol{H}\Delta\widehat{\underline{u}} \tag{7}$$

The matrices $\boldsymbol{E}$, $\boldsymbol{F}$ and $\boldsymbol{H}$ depend on the prediction horizon (N_1, N_2) and the control horizon (N_u) and are given in appendix A.

In general the optimal solution for $\Delta\widehat{\underline{u}}$ is found by solving the quadratic programming problem

$$\Delta\widehat{\underline{u}}_{\text{opt.}} = \arg \min_{\boldsymbol{M}\Delta\widehat{\underline{u}} \leq \underline{n}} \left\{ J\left(\Delta\widehat{\underline{u}}\right) \right\} \tag{8}$$

where $\boldsymbol{M}$ and $\underline{n}$ define linear constraints in the form of an inequality condition on the optimization variable $\Delta\widehat{\underline{u}}$. In the case that no constraints become relevant the solution of eq. 8 can be obtained analytically by zeroing the derivation $\partial J / \partial \Delta\widehat{\underline{u}} \stackrel{!}{=} 0$ and simplifies to a degenerated state-space control law

$$\begin{aligned} \Delta\widehat{\underline{u}}_{\text{opt.},k} &= -\left(\mathbf{I}\ \mathbf{0}\right) \left(\boldsymbol{H}^T \boldsymbol{\Gamma} \boldsymbol{H} + \boldsymbol{\Lambda}\right)^{-1} \boldsymbol{H}^T \boldsymbol{\Gamma} \cdot \widehat{\underline{e}} \\ &= -\left(\mathbf{I}\ \mathbf{0}\right) \boldsymbol{K}^*_{\text{MPC}} \cdot \widehat{\underline{e}} = \boldsymbol{K}_{\text{MPC}} \cdot \widehat{\underline{e}} \end{aligned} \tag{9}$$

with

$$\widehat{\underline{e}} = \widehat{\underline{w}} - \left(\boldsymbol{F}\underline{x}_k + \boldsymbol{E}\underline{u}_{k-1}\right) = \widehat{\underline{w}} - \widehat{\underline{y}}_{\text{free}} \tag{10}$$

where $\widehat{\underline{y}}_{\text{free}}$ is the predicted free systems response when no change of the input signal is applied to the plant. The matrix $(\mathbf{I}\ \mathbf{0})$ is used to computed $\widehat{\underline{u}}_{\text{opt.},k}$ from $\widehat{\underline{u}}_{\text{opt.}}$.

As according to eq. 10 the model-predictive controller requires the actual state $\underline{x}_k$ a Kálmán filter (see Kálmán (1960)) is designed to estimate the unmeasurable states $\widetilde{\underline{x}}_k$ using the *kalman* and *estim* functions of MATLAB/-SIMULINK®. The first function calculates the feedback matrix $\widetilde{\boldsymbol{L}}$ of the Kálmán filter, the latter is used to set up a state-space model with $\underline{u}_{\text{Obs.}} = (\underline{u}_k, \underline{y}_k)^T$ as its input and the estimated systems state $\widetilde{\underline{x}}$ as its output. The matrices $\boldsymbol{Q}$ and $\boldsymbol{R}$ which are needed for the *kalman* function and qualify the process and measurement noise respectively are - due to the lack of measured data - set to identity matrices. By this means, an even emphasis is taken on the reliability of model and measurement accuracy.

The observer matrices $\widetilde{\boldsymbol{A}}$, $\widetilde{\boldsymbol{B}}$, $\widetilde{\boldsymbol{C}}$ and $\widetilde{\boldsymbol{D}}$ are obtained by identifying the plant model with the *ident* tool of MATLAB/SIMULINK®. The processed data results from the step responses outlined in fig. 2. A system of order 12 was found adequate for observing and controlling the system.

6. RESULTS

In this section parameter studies for the introduced MPC are shown. In the following figures changes in the set-point for $\dot{m}_{\text{CCH}}$ are examined using different controller

[3] Here, no disturbance model is being applied.

parameters. The setpoints for $\xi_{O_2,CHM}$ and $\xi_{O_2,CHM}$ are constant at 15 % and 1.7 % respectively. On the left side the controlled variables $\dot{m}_{CCH}$, $\xi_{O_2,CHM}$ and $\xi_{O_2,CCH}$ are shown. The right column contains the actuating variables ω_{EBL}, ω_{CMP} and $\dot{m}_C$.

Fig. 5 shows the effect when altering the ratio $S_{\frac{\mathbf{\Lambda}}{\mathbf{\Gamma}}}$ between the weighting matrices $\mathbf{\Lambda}$ and $\mathbf{\Gamma}$ (see equation eq. 6). Increasing the ratio $S_{\frac{\mathbf{\Lambda}}{\mathbf{\Gamma}}}$ (in fig. 5 denoted with arrows) leads to heightening the penalization of moves in the actuating variables. Therefore, the controller behaviour becomes more smooth. On the other hand, the control deviation increases. With very small ratios the controller tends to overshoot and oscillate.

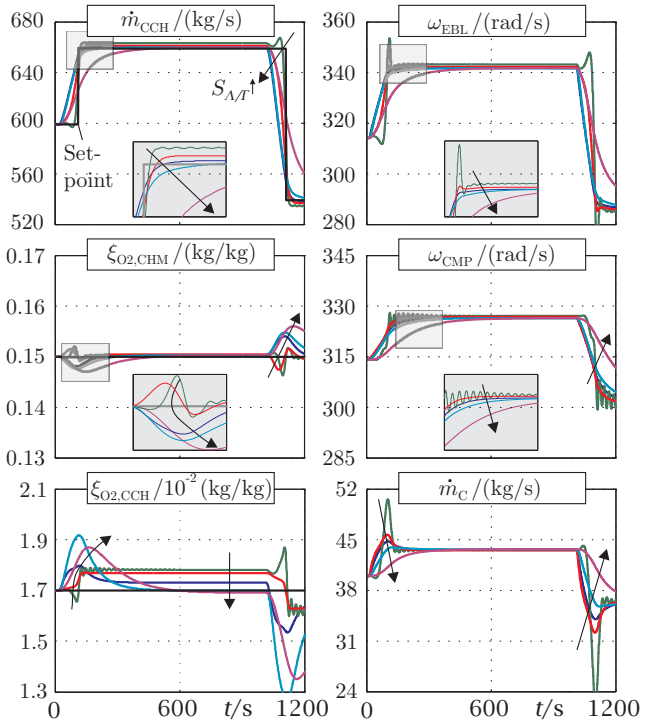

Fig. 5. Variation of $S_{\frac{\mathbf{\Lambda}}{\mathbf{\Gamma}}}$ $\left(3.5\,10^{-7}, 10^{-5}, 10^{-4}, 10^{-3}, 10^{-2}\right)$

In fig. 6 the effect of changing the weighting matrix $\boldsymbol{\gamma}$ is depicted. This matrix describes the penalization of the deviation of the controlled variables to their setpoints. Here, the penalization of deviations in $\dot{m}_{CCH}$ (i. e. y_1) is increased whereas the remaining weights are reduced. With the increase the controller realizes a smaller deviation of $\dot{m}_{CCH}$ from its setpoint at the expense of the accuracy of the left controlled variables. The more accuracy for $\dot{m}_{CCH}$ is required the stronger the actuating variables are used.

The application of a constraint on the change of the angular velocity of the compressor is shown in fig. 7. In the constrained case the angular velocity does not change faster than allowed by the constraint. Thus, limitations necessary to operate the compressor can be considered. On the other hand, the controller is restricted and higher deviations of the controlled variables occur.

The results clarify the wide range for the controller parameters which have to be chosen carefully. Furthermore, in this article just an excerpt of the possible parameters is given. Other parameters are the choice of the control

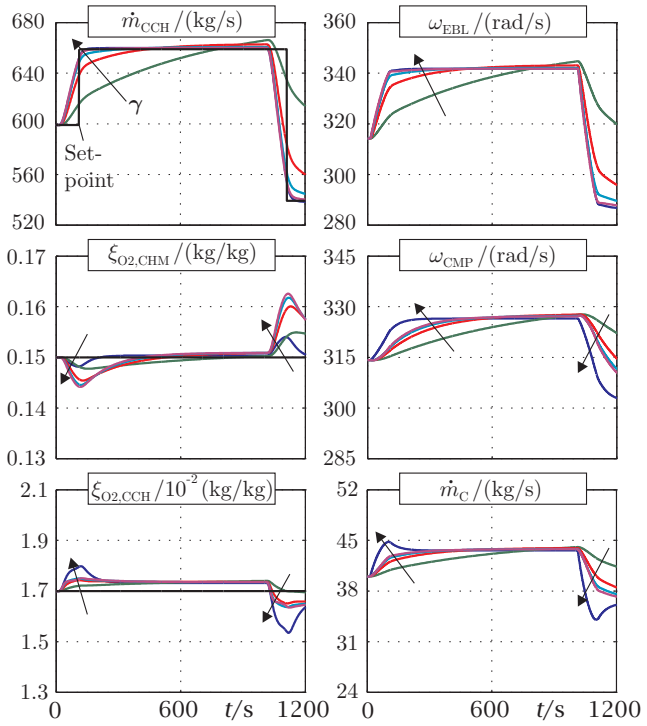

Fig. 6. Variation of γ/% $\left((9, 45, 45, 1), (33, 33, 33, 1), (60, 20, 19, 1), (80, 10, 9, 1)\right)$

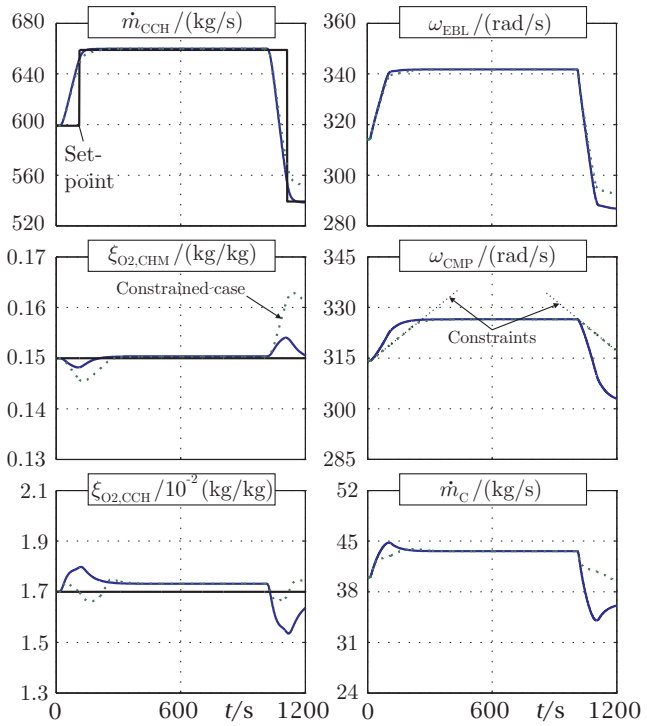

Fig. 7. Constraint on the slope of ω_{CMP}

and prediction horizon N_1, N_2 and N_u respectively, the weighting matrix $\boldsymbol{\lambda}$, the sample time T_S, constraints and others.

7. CONCLUSION

This article introduces a novel fossil power plant concept with internal carbon dioxide separation based on an oxy-

fuel combustion. A simplified model of the exhaust gas cycle is analyzed concerning control aspects. The operation of the complex and strongly coupled system makes high demands in terms of its automation, but model-predictive controllers are in particular appropriate of serving these demands.

The displayed results show a good performance of the MPC concerning changes in the setpoint. Especially the controller is capable to consider the internal coupling of the plant. The accomplished parameter studies demonstrate the effects of the controller parameters and can be used as a starting point for further research. For this reason this article makes an important contribution to the automation of the new power plant concept.

Future works will have to adapt the introduced control concept to the closed-loop exhaust gas cycle. First a disturbance model has to be applied to eq. 7 in order to realize offset free tracking. Moreover the controller will be deployed to control the nonlinear plant model. For that purpose, either the coupling between SIMULINK® and DYMOLA has to be realized or the MPC has to be implemented in DYMOLA which is straightforward in the unconstrained but elaborate for the constrained case because a solver for the latter case has to be implemented.

Furthermore, the control concept has to be integrated in the superposed control structure. Feasible sensors and actors will be explored in order to choose controlled and actuating variables.

The fundamentals depicted in this article build an excellent starting point to deal with the given aspects.

REFERENCES

J.T. Houghton, Y. Ding, D.J. Griggs, M. Noguer, P.J. van der Linden, X. Da, K. Maskell, C.A. Johnson. *Climate Change 2001: The Scientific Basis*. IPCC Third Assessment Report. http://www.grida.no/climate/ipcc_tar/.

Panel on Reconciling Temperature Observations, Climate Research Committee, Board on Atmospheric Sciences and Climate, Commission on Geosciences and Environment and Resources, National Research Council. Board on Atmospheric Sciences and Climate (BASC), editor. *Reconciling Observations of Global Temperature Change*. National Academy Press, Washington D.C., 2000. ISBN 978-0-309-06891-8.

J. A. Rossiter. *Model-Based Predictive Control: a practical approach*. CRC Press, 2003. ISBN 0-849-31291-4.

J. M. Maciejowski. *Predictive Control with Constraints*. Pearson Education Limited, 2002. ISBN 0-201-39823-0.

T. Nötges, D. Abel. Objektorientierte, nichtlineare Modellierung des Rauchgaskreislaufs eines Oxyfuel-Prozesses. In: *GMA Kongress 2007*, 12.-13.06.2007, Baden-Baden. VDI-Berichte 1980, pp. 729-738. VDI-Verlag. ISBN 978-3-18-091980-5.

N. Gašparović. Berechnung der Kennfelder mehrstufiger axialer Turbomaschinen. In: *VDI: Forschung im Ingenieurwesen* 5 (1973) 39, pp. 133-143.

C. Wagner. Equations for transport in solid oxides and sulfides of transition metals. In: *Progress in solid state chemistry* 1 (1975) 10, pp. 3-16.

F. Casella, A. Leva. Modelica open library for power plant simulation: design and validation. In: P. Fritson (editor): *Proceedings of the 3rd International Modelica conference*, Linköpings, Schweden, 2003.

F. Casella, M. Otter, K. Proelss, C. Richter, H. Tummescheit. The Modelica Fluid and Media Library for Modeling of Incompressible and Compressible Thermo-Fluid Pipe Networks. In: *Proceedings of the 5th International Modelica Conference*, pp.631-640. Vienna, Austria, 4-5 September 2006.

R. E. Kálmán. A new approach to linear filtering and prediction problems. In: *Journal of Basic Engineering* 1 (1960) 82, pp. 34-45.

T. Nötges, S. Hölemann, N. Bayer Botero, D. Abel. Objektorientierte Modellierung, Simulation und Regelung dynamischer Systeme am Beispiel eines Oxyfuel-Kraftwerksprozesses. In: *at-Automatisierungstechnik* 55 (2007) 15, pp. 236-243. Oldenbourg Verlag.

Appendix A. USED MATRICES AND VECTORS

The input and output vectors are built:

$$\underline{u}_k = \begin{pmatrix} \omega_{\mathrm{EBL}} \\ \omega_{\mathrm{CMP}} \\ \dot{m}_{\mathrm{C}} \end{pmatrix}, \; \underline{y}_k = \begin{pmatrix} \dot{m}_{\mathrm{CCH}} \\ \xi_{\mathrm{O_2,CHM}} \\ \xi_{\mathrm{O_2,CCH}} \end{pmatrix}. \tag{A.1}$$

The structure of the matrices used for the MPC is:

$$\boldsymbol{F} = \begin{pmatrix} \boldsymbol{C}\boldsymbol{A}^{N_1} \\ \vdots \\ \boldsymbol{C}\boldsymbol{A}^{N_2} \end{pmatrix}, \tag{A.2}$$

$$\boldsymbol{E} = \begin{pmatrix} \sum_{i=0}^{N_1-1} \left(\boldsymbol{C}\boldsymbol{A}^i\boldsymbol{B}\right) + \boldsymbol{D} \\ \vdots \\ \sum_{i=0}^{N_2-1} \left(\boldsymbol{C}\boldsymbol{A}^i\boldsymbol{B}\right) + \boldsymbol{D} \end{pmatrix} \tag{A.3}$$

and

$$\boldsymbol{H} = \begin{pmatrix} \boldsymbol{h}_{N_1-1} & 0 & \dots & \dots & \dots & 0 \\ \boldsymbol{h}_{N_1} & \boldsymbol{h}_{N_1-1} & \ddots & & & \vdots \\ \vdots & \ddots & \ddots & \ddots & & \vdots \\ \vdots & & \ddots & \ddots & \ddots & \vdots \\ \vdots & & & \ddots & \ddots & 0 \\ \boldsymbol{h}_{N_u-1} & & & & \ddots & \boldsymbol{h}_{N_1-1} \\ \boldsymbol{h}_{N_u} & \ddots & & & & \boldsymbol{h}_{N_1} \\ \vdots & \ddots & \ddots & & & \vdots \\ \boldsymbol{h}_{N_2-1} & \dots & \boldsymbol{h}_{N_u} & \boldsymbol{h}_{N_u-1} & \dots & \boldsymbol{h}_{N_2-N_u-1} \end{pmatrix} \tag{A.4}$$

with

$$\boldsymbol{h}_{n-m} = \begin{cases} \sum_{i=0}^{n-m} \left(\boldsymbol{C}\boldsymbol{A}^i\boldsymbol{B}\right) + \boldsymbol{D} & n-m \geq 0 \\ 0 & n-m < 0. \end{cases} \tag{A.5}$$